

Electron Microscopy of Multi-walled Carbon Nanotubes for Display Devices Application

P. Ghosal¹, R. Sarkar¹, K. Muraleedharan¹, P. Chaturvedi², J.S.B.S. Rawat², and Harsh²

¹Defence Metallurgical Research Laboratory, Hyderabad-500 058

²Solid State Physics Laboratory, Delhi-110 054

ABSTRACT

The opportunity of creating and tailoring unprecedented and beautifully symmetric 3-D structures has propelled the science of carbon nanotubes to become one of the highly promising areas in the field of nanotechnology. The unique properties of carbon nanotubes have promoted research in the fabrication of devices composed of carbon nanotubes and in other applications. Characterisation tools are crucial in the study of these emerging materials to evaluate their full potential in applications and to comprehend their basic properties. The aim of this study was electron microscopy characterisation of the carbon nanotubes synthesised to fabricate display devices. Both thermal chemical vapour deposition (CVD) and plasma enhanced chemical vapour deposition routes were used to synthesise patterned and aligned carbon nanotubes. Several batches of CNTs were produced by varying the process parameters such as growth temperature, gas ratio, duration of growth, catalyst condition, etc. Characterisation of these CNTs have been done using scanning electron microscope, transmission electron microscope, high resolution transmission electron microscope, and electron energy loss spectrum. Structure, uniformity, chemistry, diameter, length, number of walls of the multi-walled nanotubes were characterised using various electron microscopes, which finally lead to the production of the display devices using CNTs.

Key words: Carbon nanotubes, HRTEM, electron energy loss spectrum, EELS, thermal chemical vapour deposition, plasma-enhanced chemical vapour deposition, PECVD

1. INTRODUCTION

The remarkable properties of carbon nanotubes (CNTs) with wide range of anticipated applications have prompted extensive research in this field since their discovery by Iijima in 1991¹. A CNT can simply be viewed as a one-dimensional fullerene with a cylindrical shape or as a rolled up graphite sheet. Carbon nanotube has essentially sp^2 carbon-carbon bonding. The circular curvature of CNT will cause $\sigma\pi$ rehybridization in which three σ bonds are slightly out of plane, resulting the π orbital more delocalised outside the tube. The CNT in general can be classified as single-walled nanotube (SWNT) and multi-walled nanotube (MWNT). A SWNT can be visualised as a hollow cylinder formed by the rolling of a graphite sheet whereas a MWNT can be considered to be a coaxial assembly of cylinders of SWNTs. Depending upon the nature of rolling, i.e., chiral angle, the carbon can be classified in three types: zigzag ($\theta = 0$, $m = 0$), armchair ($\theta = 30^\circ$, $m = n$) and chiral ($0 < \theta < 30^\circ$) nanotubes.

The CNT was first produced by arc discharge method¹ but it can also be synthesised by laser ablation and chemical vapour deposition (CVD) technique. In arc discharge process, carbon nanotubes are prepared by striking a direct current arc between graphite electrodes in an inert atmosphere of helium or argon gas. In laser ablation method, a piece of graphite target is vapourised by laser irradiation under high

temperature in an inert atmosphere. The CVD method is a continuous gas-phase process working on the principle^{2,3} of cracking and decomposition of the carbon source gas such as benzene, methane, acetylene, and carbon monoxide, molecules at high temperature over the catalyst, which is on the substrate. In case of plasma-enhanced carbon vapour deposition (PECVD)^{2,4}, the precursor is dissociated by highly energetic electrons and as a result, substrate temperature can be substantially lower than that in the case of thermal CVD. Carbon nanotubes are also synthesised by high pressure carbon monoxide (HiPco) process, diffusion flame synthesis, electrolysis using graphite electrodes immersed in molten ionic salts, ball milling of graphite, and heat treatment of a polymer⁵.

The CNTs possess excellent mechanical properties. Theoretical and experimental works on carbon nanotubes have confirmed that these are one of the stiffest materials ever made and strong carbon-carbon covalent bonds make it one of the strongest materials also. The SWNTs possess Young's modulus of the order of 1.05 TPa while the MWNTs possess 1.2 TPa in comparison to 0.21 TPa of steel⁶. In addition to these mechanical properties, carbon nanotubes possess high chemical and thermal stability. The most exiting of nanotube properties relates to its electronic band structure. Many potential applications based on the unique electronic structure, mechanical strength, flexibility, and dimensions

of nanotubes have been proposed for the CNTs, including conductive and high-strength composites, energy storage and energy conversion devices, sensors, field emission displays and radiation sources, hydrogen storage media, and nanometer-sized semiconductor devices, probes, and interconnects. Some of these applications are now realised in products.

In the present work, the CNTs are synthesised by CVD and PECVD processes mainly for device applications like field emission displays, cold cathodes, etc. But to have a clear knowledge on structure-property correlation of CNTs for device applications, characterisations are very important. Correlation of characterisation of microstructures with properties is important to understand what is controlling the properties and structures of materials and their relation with processing conditions. Detailed electron microscopy characterisations on the thickness of walls, number of walls, bore, uniformity, entrapped particles, bending of carbon nanotubes have been carried out to correlate these with growth processes.

2. EXPERIMENTAL DETAILS

2.1 Synthesis

The CNTs were synthesised both by thermal CVD and PECVD techniques. Thermal CVD route was carried out using in-house developed thermally-heated CVD reactor having 40 mm dia quartz reactor tube. A schematic view of the furnace used is shown in Fig. 1. The CNTs were grown on a substrate composed of four layers. The lowermost one was *n*-type *Si* (100) substrate of resistivity (ρ) 4-6 Ωcm which was pre-cleaned to remove any greasy material from the surface. On the *Si* substrate there were consecutive layers of SiO_2 , *Cr*, and SiO_2 , respectively. Iron catalyst film was deposited on to the substrate using standard RF sputtering technique. To achieve selective vertically aligned growth of the carbon nanotubes with optimum nanotip density, the catalyst-deposited substrate was patterned using

photolithography followed by lift-off to retain iron islands of 20 μm and 100 μm dia on to the substrate with varying spacing. A continuous film of *Fe* was also used as a different substrate for growing CNTs. Argon gas was passed through the quartz tube to prevent the oxidation of the catalytic material as the furnace was heated to operating temperature. After cleaning of the patterned substrate, the growth of the CNTs was carried out using NH_3 and C_2H_2 mixture. Growth temperatures were maintained at 1123 K and 1023 K for different cases. Different samples prepared for characterisation by varying the processing parameters such as growth temperature, growth duration, gas ratios, and catalyst, are described in Table 1. The gaseous products, obtained besides the deposited carbon due to the reaction, were taken out through exhaust nozzle. The CNTs were grown selectively by PECVD at temperature < 939 K over *Si* substrate. This experiment was carried out in a capacitively coupled, RF (13.56 MHz) hot filament PECVD system based on SS-cross-type chamber. Catalyst patterns of 20 μm *Fe* (catalyst) dots were made over *n*-*Si* (100) by photolithography followed by sputtering and lift-off. After loading *Fe*-patterned substrate, chamber was initially evacuated to 10-5 Torr by DP. It was then put on rotary pumping and pressure was maintained at 5 Torr using H_2 purging at 50 sccm. After 30 min, H_2 was stopped followed by striking of plasma between electrodes. Heating was immediately started in NH_3 flow of 100 sccm. After reaching 873 K, additional NH_3 plasma treatment for few minutes was given to break *Fe* particles into small islands. The CNTs growth was carried out using C_2H_2 and NH_3 for 10 min and substrate was cooled in N_2 ambience.

2.2 Characterisation

Synthesised CNTs were characterised using Leo 440i SEM (with EDAX). Nanotubes with the substrate were

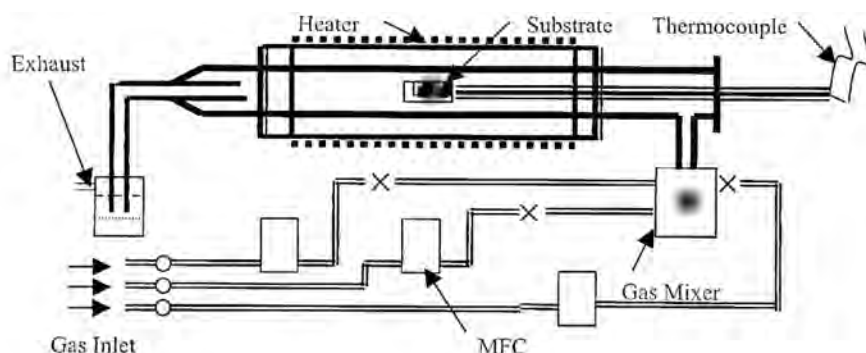


Figure 1. Schematic view of the furnace used for CNT growth by thermal CVD process.

Table 1. Different samples synthesised by varying processing for characterisation

Catalyst used	Growth temperature (K)	Growth duration (min)	Gas ratio (C_2H_2 : NH_3)	Sample code
<i>Fe</i> (continuous)	1123	8	1:1	FC123
<i>Fe</i> (continuous)	1023	12	1:10	FC023
<i>Fe</i> (20 mm dots)	1123	8	1:4	F2123
<i>Fe</i> (20 mm dots)	1023	12	1:10	F2023
<i>Fe</i> (20 mm dots)	873	10	-	PECVD

stuck on a brass stub and introduced in the SEM. Electron microscopy of CNTs was done using Tecnai G2 AEM and Tecnai UT HRTEM with GATAN image filter. Sample preparation for electron microscopy characterisation required lifting-off the CNTs from the substrate which was done by scraping the substrate with blade (Fig. 2) Lifted-off CNTs were then put into methanol and the tubes were separated by ultrasonic vibration. Separated CNTs were then lifted on carbon grid and introduced in the electron microscope for characterisation. A number of TEM and HRTEM micrographs were observed for the understanding of different aspects of CNTs. During the characterisation of the nanotubes



Figure 2. Substrate has been scraped with blade to lift off carbon nanotubes for sample preparation for electron microscopy characterisation.

using electron microscopes, it is difficult to work on any particular area as nanotubes get transformed to amorphous after long exposure to electron beam.

3. RESULTS AND DISCUSSION

The CNTs synthesised at SSPL, Delhi, were grown in patterned and aligned manner as it was aimed for the application of display device. SEM micrographs of patterned and aligned growth of the CNTs are shown in Fig. 3. High magnification SEM micrograph in Fig. 4 is showing spaghetti like columnar growth of MWCNTs. The SEM micrographs reveal high density of CNTs. When the density of nanotubes reaches a high value, nanotubes grown in direction other than the vertical direction are prohibited from growing due to crowding effect, i.e., neighbouring tubes supporting each other by

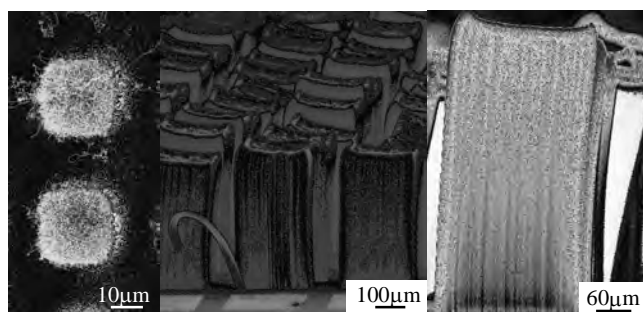


Figure 3. Typical SEM micrographs of patterned and aligned carbon nanotubes.

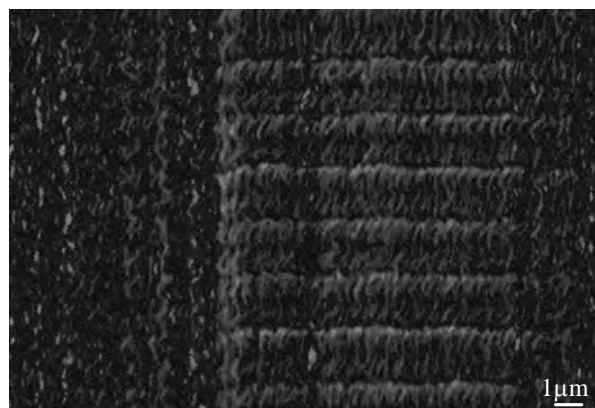


Figure 4. SEM micrograph showing spaghetti like columnar growth of multi-wall carbon nanotubes.

van der Waals force and thereby become vertically aligned⁷. But, individual CNTs within the ensemble grow almost like vines even though the ensemble looks nicely aligned. A low magnification TEM micrograph (Fig. 5) shows a forest of CNTs of FC123 sample with encapsulated particles at

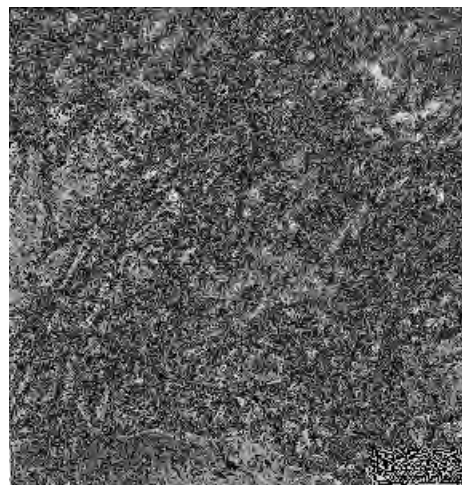


Figure 5. Low magnification TEM micrograph showing a forest of carbon nanotubes sample with encapsulated particles at the nanotube tip.



Figure 6. High magnification TEM micrograph showing a large particle at the tip of a nanotube.

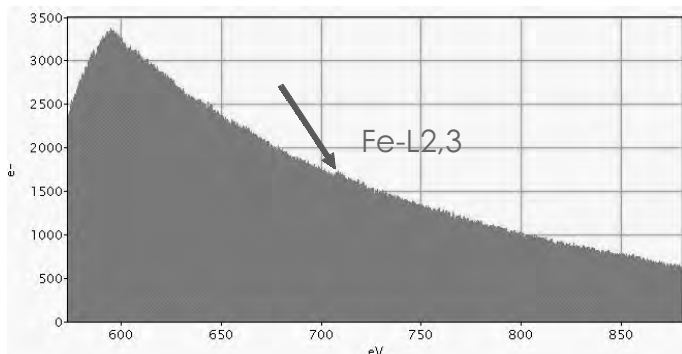


Figure 7. Electron energy loss spectrum study of the particle at tip of nanotubes showing Fe peak.

the nanotube tip. A high magnification TEM micrograph (Fig. 6) shows a large particle at the tip of a nanotube and the particle was further examined to be Fe and FeO. Both electron energy loss spectrum (EELS) (Fig. 7) and EDAX study (Fig. 8) of the particle at the tip confirm the presence

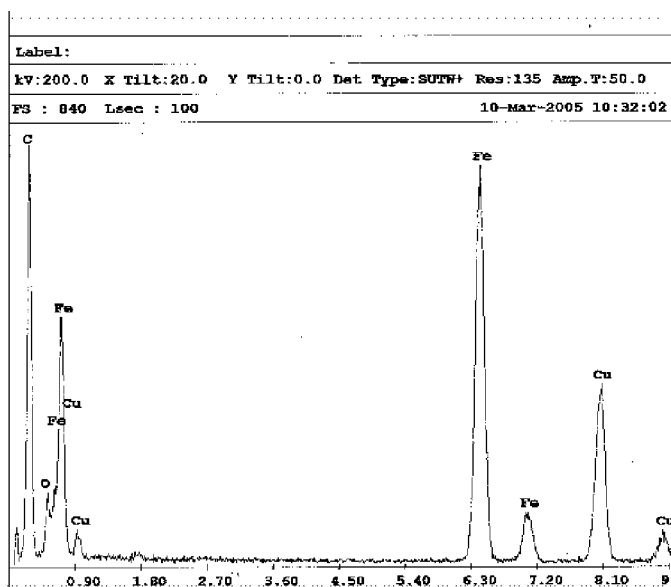


Figure 8. EDAX study of the particle at the tip of the nanotubes showing peaks of Fe and O, other than C and Cu which are coming from CNT and Cu grid respectively.

of Fe and in some cases FeO at the tip of CNT. Selected area diffraction (SAD) from the tip (Fig. 9) also confirms the presence of Fe by showing Fe diffraction spots. The size of the tip is in nanorange, as a result the diffraction rings are forming along with spots. Higher magnification HRTEM micrograph (Fig. 10) reveals the lattice fringes of a particle at the tip and lattice spacing was calculated as 1.8 Å which matches well with (024) plane of FeO.

High-resolution TEM micrographs (Fig. 11) of a PECVD sample shows the walls of a CNTs curved around the encapsulated Fe particle and it also reveals separation between the walls at the tip. Typical high magnification HRTEM micrographs (Fig. 12) of a F2123 sample divulge the well-ordered lattice fringes of the nanotubes. The number of walls forming the nanotube as found from the micrographs was in the range 27–35. It is measured from

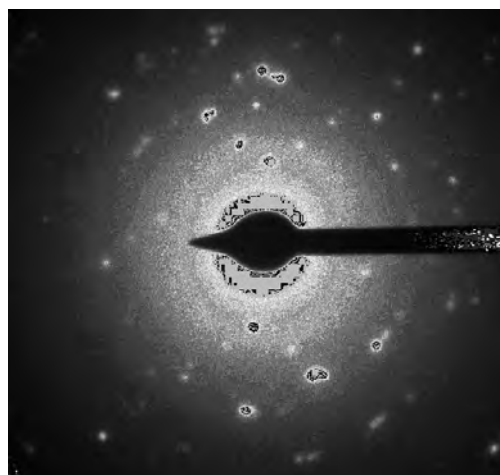


Figure 9. Selected area diffraction from the nanotubes tip showing Fe diffraction spots.

Fig. 12 that the planes have a lattice spacing around 3.6 Å, which matches well with (002) planes of carbon. It can be observed from a typical TEM micrograph of a PECVD sample (Fig. 13), that CNTs appear to grow in different directions from a lump of catalyst. Figure 13 also reveals that the tubes grown have different diameters. The CNTs processed in different condition, and even in the same condition, might have different diameters. Nanotubes of

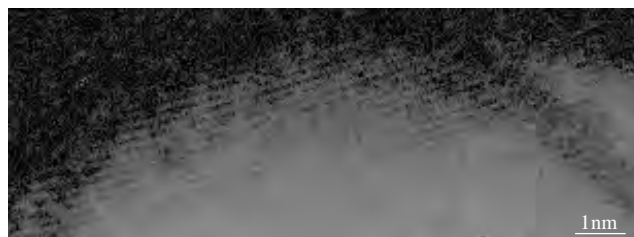


Figure 10. High magnification micrograph of a particle at nanotube tip reveals the lattice fringes of the particle.

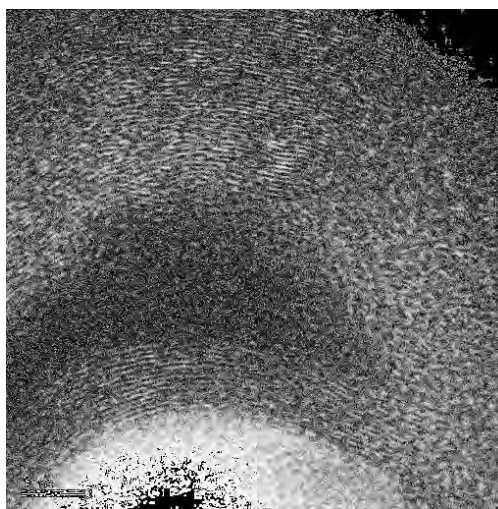


Figure 11. High-resolution TEM micrograph of a PECVD sample showing the walls of a carbon nanotube curved around the encapsulated Fe particle.

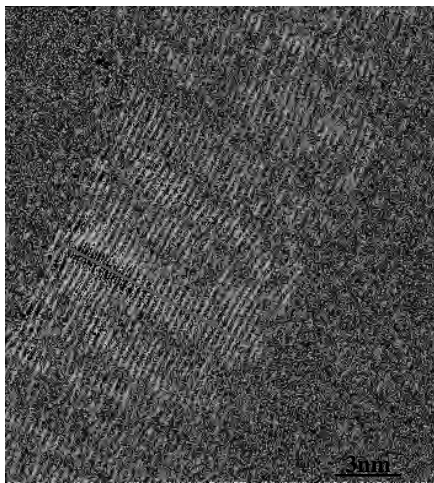


Figure 12. High magnification HRTEM micrograph divulging the well ordered lattice fringes of the nanotubes.

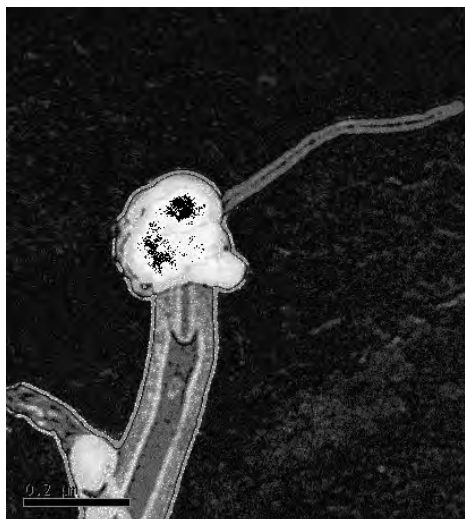


Figure 13. Typical TEM micrograph of a PECVD sample showing carbon nanotubes growing in different direction from a lump of catalyst.

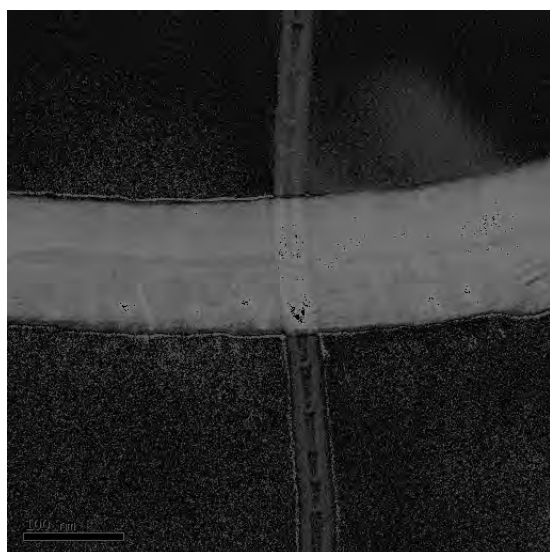


Figure 14. Carbon nanotubes processed in identical condition (FC023 sample) having different diameters.

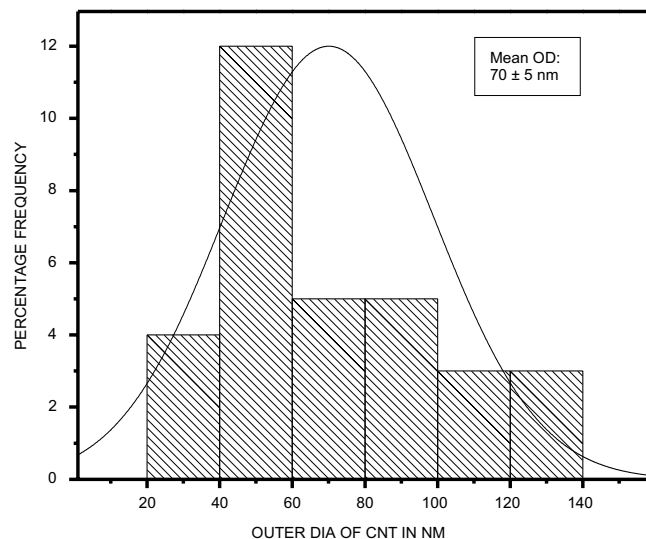


Figure 15. Comparative result of diameters of carbon nanotubes processed in different conditions.

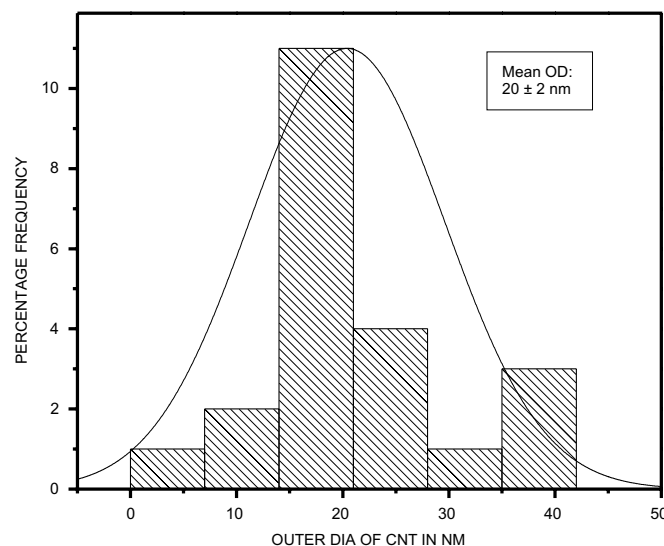


Figure 16. Statistical plot of measured inner diameter of CNTs for FC023 sample.

different diameters for FC023 sample are shown in Fig. 14. Diameters of CNTs were measured on number of tubes for different samples and for FC023 sample, the average outer diameter was found to be 70 ± 5 nm. Figure 15 shows a statistical plot of measured outer diameter of FC023 sample, while Fig. 16 shows the same for inner diameter of FC023 sample. A comparative result of diameters of CNTs processed in different conditions is shown in Fig. 17 and depicted in Table 2. It was observed from measured diameter of nanotubes that average diameter of nanotubes changes with process conditions. Comparing the average diameters of CNTs, which were grown on continuous *Fe* catalyst, it was noticed that CNTs of FC123 sample have smaller diameters than those of sample FC023. This decrease in diameter might be due to increase in growth temperature but could not be confirmed as gas ratio also varied for different processes. Increase in growth temperature reduces grain size⁸ by shattering the continuous

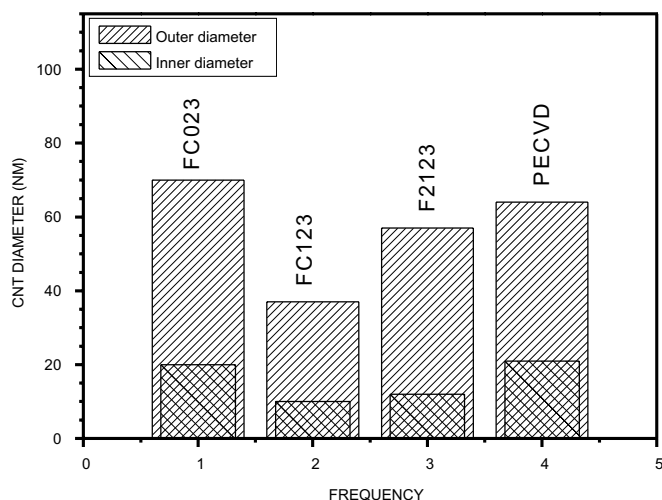


Figure 17. Comparative result of diameters of carbon nanotubes processed in different conditions.

film of catalyst and also increases surface roughness⁹ of the particles. Therefore, increase in growth temperature can reduce CNT diameter, as diameter of CNTs are directly proportional to catalyst particle size. The NH_3 pre-treatment of catalyst particle also has an effect on diameter and density of CNTs, because NH_3 etches the surface of catalyst particle and provides better nucleation sites^{8,10,11}. But, overtreatment with NH_3 may increase tube diameter as it forms agglomerate of particles¹¹. It can be observed from Figs 18 and 19 that CNTs of FC123 sample have higher density than those of FC023 sample. Lower density of CNTs of FC023 sample may be attributed to the relatively lower growth temperature and higher percentage of NH_3 usage due to the above-mentioned reasons. It can also be noticed from Figs 18 and 19 that CNTs of FC123 sample are longer than those of FC023 sample. Average length

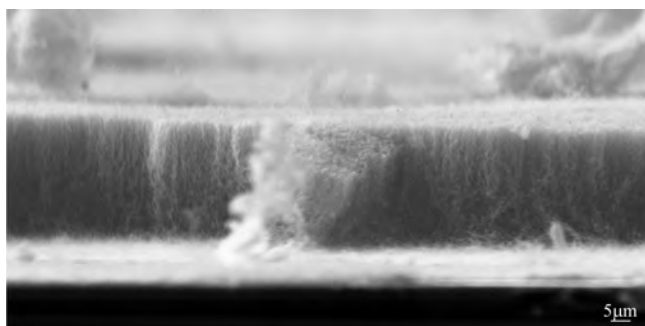


Figure 18. SEM micrograph of CNTs of FC123 sample showing aligned growth of tubes and their density.

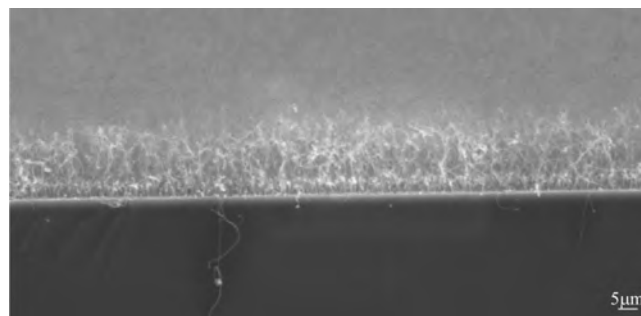


Figure 19. SEM micrograph of CNTs of FC023 sample showing aligned growth of tubes and their density.

of FC123 CNT is 17μ and that of FC023 CNTs is 9μ , as shown in Table 2. Therefore, length of CNTs increases with decrease in diameter which is similar to the observation of Lee¹¹, *et al.* This phenomenon can be better described in terms of growth rate. Growth rate of CNTs of FC123 sample is $2.1 \mu/min$ while that of FC023 sample is $0.8 \mu/min$. Growth rate of tubes is inversely related to tube diameter¹² and it also increases with decrease in catalyst particle size¹³. As the size of particle decreases, diffusion time for carbon to arrive at growth site become short, resulting in accelerating the growth rate of CNTs¹¹. In brief, it is observed that with increase in growth temperature, CNT diameter decreases, length and density increase. Cui⁹, *et al.* have reported that CNT length and density increases with initial increase in growth temperature, but with further increase

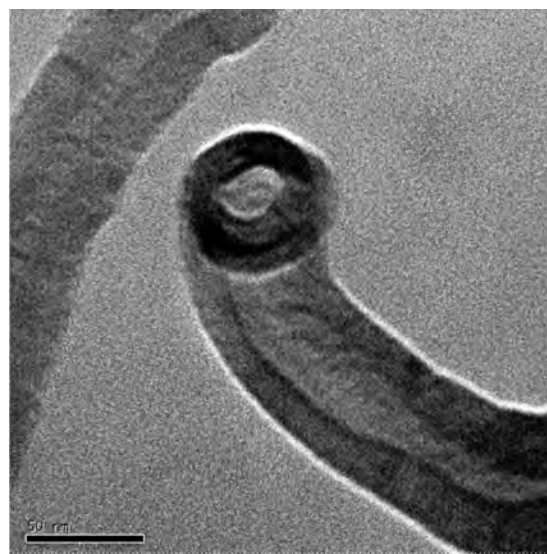


Figure 20. TEM micrograph showing a hanging open-end MWNT.

Table 2. Diameters, length and growth rate of CNTs processed in different conditions

Sample code	Average outer diameter (nm)	Average inner diameter (nm)	Average length (μ m)	Growth rate (μ m/min)
FC123	37 ± 4	10 ± 1	17	2.1
FC023	70 ± 5	20 ± 2	9	0.8
F2123	57 ± 3	12 ± 4	11	1.4
PECVD	64 ± 12	21 ± 6	-	-

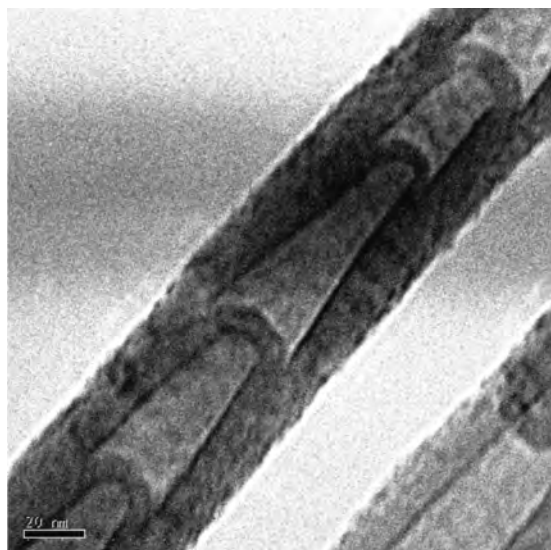


Figure 21. TEM micrograph showing bamboo structured MWNT with closed internal cap.

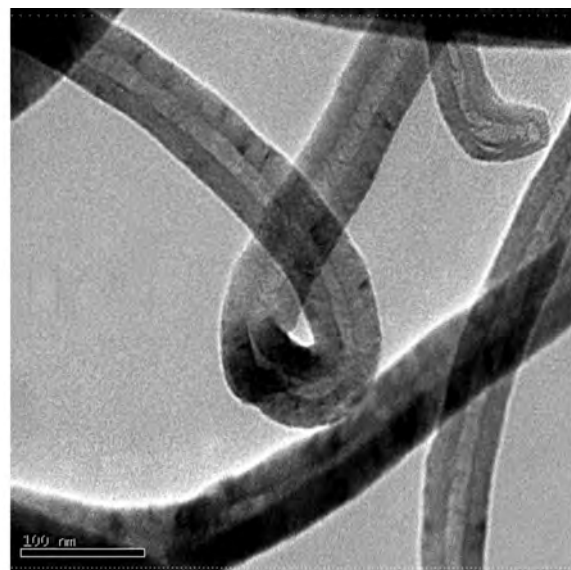


Figure 23. TEM micrograph showing bent carbon nanotubes.

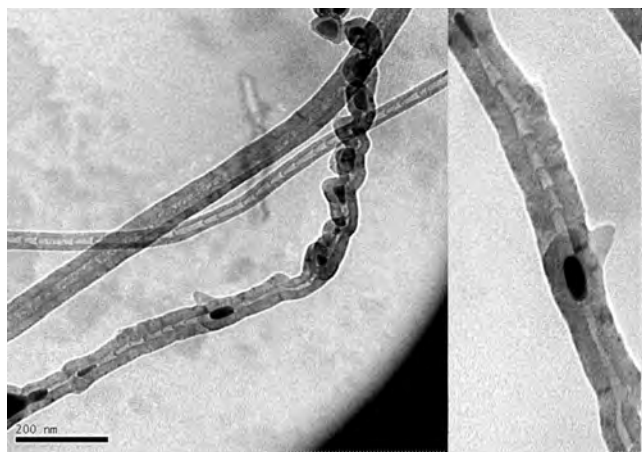


Figure 22. Non-uniform growths of CNTs and Fe entrapped in different positions of the MWNT.

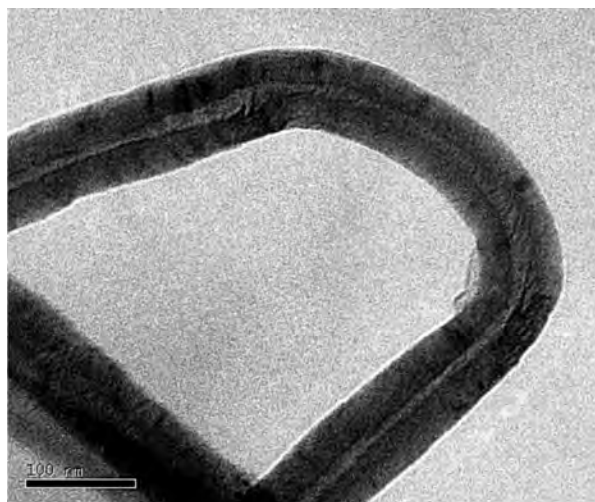


Figure 24. TEM micrograph showing a 'U' type bend of carbon nanotube.

in temperature, length and density start decreasing.

The CNTs of different types such as open-structured, closed-MWNT with internal cap, bamboo-structured MWNT, bent-structured were observed during the characterisation. Figure 20 shows a hanging open end MWNT (F2023) having outer diameter of 50 nm. Bamboo-structured MWNT with closed internal cap was observed for FC023 specimen as shown in Fig. 21. This bamboo structure might be due to the bulk diffusion of carbon in the catalyst¹⁰. Wang¹⁴, *et al.* have reported that thick film of catalyst with larger island (catalyst particles) diameter produces CNTs with larger dia. These CNTs possess bamboo like structures as surface and bulk diffusions are comparable in this condition. But, a hollow structure would be formed for smaller diameter CNTs nucleated on small particles, because surface diffusion predominates. Figure 22 reveals non-uniform growth of CNT and Fe entrapped in different positions of the MWNT. Bent carbon nanotubes were also characterised as shown in Fig. 23 for FC023 specimen.

The fact is that graphite is by itself a very brittle material, but predominantly MWNT and sometimes SWNT in the TEM appear to indicate that these are resilient, i.e., capable of high level of bending and torsional stress prior to fracture. U type bend and V type bend nanotubes were observed for F2023 and FC123 specimens as shown in Figs 24 and 25. Simulation of bending mechanism¹⁵ in SWNTs shows compressive/tensional areas with sharp edges; whereas bending mechanism observed for MWNTs in the present study do not follow as in SWNTs. Damages in the wall of MWNTs can be observed in compressive and tensional areas, but walls of tubes do not collapse or generate sharp edges due to bending. This observation needs modelling support to explain.

Upon characterisation, all the CNTs processed in different conditions, the one processed through PECVD route was chosen for fabricating display devices. Using the PECVD-processed, CNTs, alphanumeric display as shown in Fig. 26 have been developed.

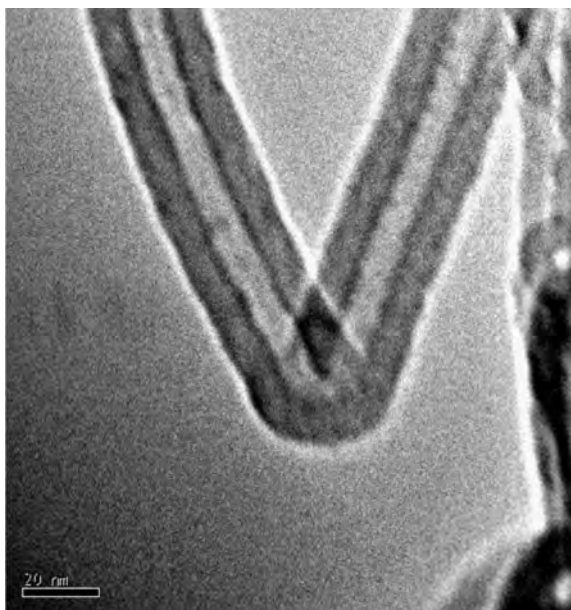


Figure 25. TEM micrograph showing a 'V' type bend of carbon nanotube.

particles were observed at the tip of the tube confirming tip growth phenomenon. In some cases, particles inside the body of the tubes were also observed and these conditions were rejected. Average diameters, length, growth rate of the tubes were measured and it was observed that tubes synthesised at high growth temperature have lesser diam and more length. Bending of the MWNTs were also observed during characterisation but no collapses or sharp edges in the walls were observed like SWCNTs. Damages in the wall of MWNTs were observed in compressive and tensional areas, but walls of tubes did not collapse or generate sharp edges due to bending. Degradation of field emitters is an important issue for the device performance and thus non-uniformity of nanotube tips is one of the degradation mechanisms. Therefore to characterise the nanotube structure, uniformity, impurity, and chemistry electron microscopes are the most worthy instruments. The CNTs processed by PECVD route gave more uniform structures than by others routes. These CNTs were used for the fabrication of flat-panel display devices as a feasibility project, demonstrated as shown in Fig. 26.

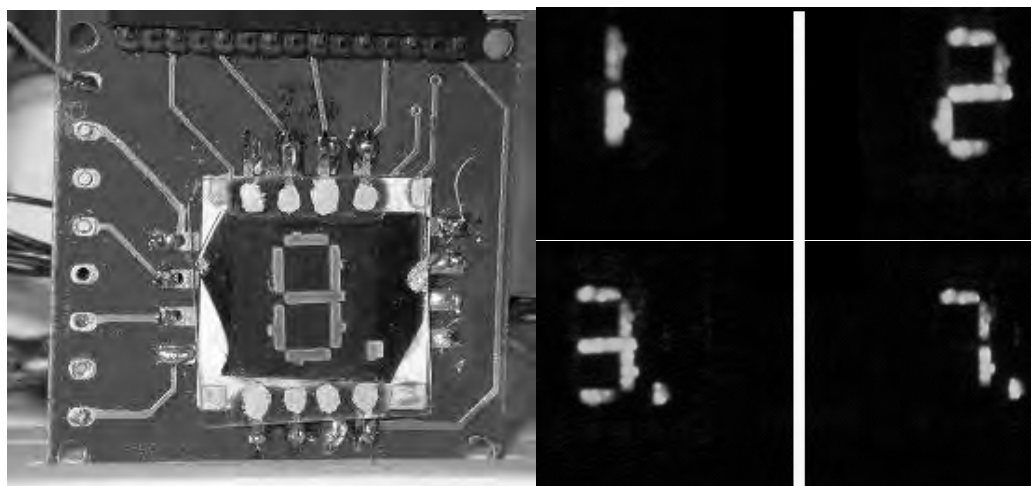


Figure 26. CNT-based flat panel display produced at SSPL, Delhi.

4. CONCLUSIONS

Primary object of this study was to synthesise and characterise CNTs processed in different conditions for fabricating display devices. Characterisation of these CNTs has been done using SEM, TEM, HRTEM, and EELS. Major requirement for flat-panel display is to grow CNTs vertically aligned and patterned. The SEM characterisation clearly showed the patterned and aligned growth of the tubes. TEM and HRTEM characterisation of the CNTs revealed the condition of the walls and number of the walls present in the tube. In most of the cases, tube walls were well graphitised but not for all. Two major types of nanotubes: (a) bamboo-structured closed internal cap and (b) hollow multi-walled *Fe* capped and encapsulated tubes with mostly uniform and non-uniform walls, have been observed during characterisation.

It was noticed that for almost all the cases, catalyst

ACKNOWLEDGEMENTS

The authors thank Dr D. Banerjee, CCR&D (AMS) and Dr A.M. Sriramamurty for their constant support and encouragement. They would also like to thank Dr G. Malakondaiah, Director, DMRL, Hyderabad, for his permission to publish this work and DRDO for financial assistance.

REFERENCES

1. Iijima, S. Helical microtubules of graphitic carbon. *Nature*, 1991, **354**, 56-58.
2. Meyeppan, M. Growth: CVD and PECVD. In *Carbon nanotubes science and applications*, edited by M. Meyeppan. CRC Press, US, 2005. pp. 99-116.
3. Dupuis, A. The catalyst in the CCVD of carbon nanotubes—a review. *Progress Mater. Sci.*, 2005, **50**, 929-61.
4. Ho, G.W.; Wee, A.T.S.; Lin, J. & Tjiu, W.C. Synthesis of well-aligned multiwalled carbon nanotubes on *Ni*

- catalyst using radio frequency plasma-enhanced chemical vapour deposition. *Thin Solid Films*, 2001, **388**, 73-77.
5. Awasthi, K.; Srivastava, A. & Srivastava, O.N. Synthesis of carbon nanotubes. *J. Nanosci. Nanotech.*, 2005, **5**(10), 1616-636.
 6. Han, J. Structures and properties of carbon nanotubes. *In Carbon nanotubes science and applications*, edited by M. Meyeppan. CRC Press, US, 2005. pp. 1-24.
 7. Srivastava, S.K.; Vankar, V.D. & Kumar, V. Growth and microstructures of carbon nanotube films prepared by microwave plasma enhanced chemical vapour deposition process. *Thin Solid Films*, 2006, **515**(4), 1552-560.
 8. Lee, C.J.; Han, J.H.; Yoo, J.E.; Kang, S.Y.; Lee, J.H. & Cho, K. Well-aligned carbon nanotubes grown on large-area Si substrate by thermal chemical-vapour deposition. *J. Korean Physical Soc.*, 2000, **37**(6), 858-61.
 9. Cui, H.; Eres, G.; Howe, J.Y.; Purotky, A.; Varela, M.; Geohagan, D.B. & Lowndes, D.H. Growth behaviour of carbon nanotubes on multilayered metal catalyst film in chemical vapour deposition. *Chemical Phys. Lett.*, 2003, **374**, 222-28.
 10. Lee, C.J.; Park, J.H. & Park, J. Synthesis of bamboo-shaped multiwalled carbon nanotubes using thermal chemical vapour deposition. *Chemical Phys. Lett.*, 2000, **323**, 560-65.
 11. Lee, C.J.; Lyu, S.C.; Cho, Y.R.; Lee, J.H. & Cho, K.I. Diameter-controlled growth of carbon nanotubes using thermal chemical vapour deposition. *Chemical Phys. Lett.*, 2001, **341**, 245-49.
 12. Bower, C.; Zhou, Zhu, O. W.; Werder, D.J. & Jin, S. Nucleation and growth of carbon nanotubes by microwave chemical vapour deposition. *Appl. Phys. Lett.*, 2000, **77**, 2767-769.
 13. Choi, Y.C.; Shin, Y.M.; Lee, Y.H.; Lee, B.S.; Park, G.S.; Choi, W.B.; Lee, N.S. & Kim, J.M. Controlling the diameter growth rate, and density of vertically aligned carbon nanotubes synthesised by microwave plasma enhanced chemical vapour deposition. *Appl. Phys. Letters*, 2000, **76**, 2367-369.
 14. Wang, Y.Y.; Gupta, S.; Nemanich, R.J.; Liu, Z.J. and Qin, L.C. Hollow to bamboolike internal structure transition observed in carbon nanotube films. *J. Appl. Phys.*, 2005, **98** (014312), 1-6.
 15. Ajayan, P. Carbon nanotubes. *In Nanostructured materials and nanotechnology*, edited by H.S. Nalwa. Academic Press, US, 2002. pp. 329-60.

Contributors



Dr Partha Ghosal Sci E at Defence Metallurgical Research Laboratory (DMRL), Hyderabad, obtained his PhD in Metallurgical Engg from Banaras Hindu University, Varanasi. His fields of specialisation are: Nano materials characterisation, defects/faults characterisation, intermetallic compounds, structure determination, and electron microscopy.

He has about 30 papers and 40 presentations in conferences and one patent to his credit. He is life member of various professional societies.



Mr Rajdeep Sarkar is Sci C at DMRL, Hyderabad. He obtained his MTech in Metallurgical Engg from IIT, Kharagpur. His fields of specialisation include: Characterisation using scanning electron microscope (SEM), environmental scanning electron microscope (ESEM), dual-beam SEM, transmission electron microscope (TEM), high resolution TEM (HRTEM),

and *in-situ* nanoindentation in TEM. He has seven published papers eight conference presentations and three technical reports to his credit.



Dr K. Muraleedharan obtained his BTech and PhD both from Banaras Hindu University, Varanasi. At present, he is Head, Electron Microscopy Division at DMRL, Hyderabad. Before this assignment, he worked at Midhani, Hyderabad, during 1983-1984. He was also Research Faculty at Carnegie Mellon University, Pittsburg, USA. His research interests include: Science and design of advanced materials, and

multi-scale microstructural characterisation using techniques such as transmission electron microscopy and 3-D atom probe field ion microscopy, as applied to the study of electronic materials and solid-state phase transformations.

Mr Poornendu Chaturvedi (see page 599)

Mr J.S.B.S. Rawat (see page 654)

Dr Harsh (see page 599)